Korean J. Chem. Eng., 40(7), 1767-1774 (2023)
DOI: 10.1007/s11814-023-1436-9

pISSN: 0256-1115
eISSN: 1975-7220

Investigation on the adsorption performance of modified coal gangues to p-hydroxybenzenesulfonic acid

Longgui Peng†, Rong Wang, Huanquan Cheng, Liangqing Zhang, Yugang He, Chenghui Yin, and Xin Zhang

College of Materials Science & Engineering, Xi'an University of Science and Technology, Xi'an, 710054, China
(*Received 1 December 2022 • Revised 3 February 2023 • Accepted 5 February 2023*)

Abstract−Coal gangue (CG) has dense structure and excellent internal crystallization. After modification, its pore structure can be enlarged and become an adsorptive material with good adsorption performance, which is a good idea to recover solid waste of CG to a certain extent. At the same time, the content of organic matter in the wastewater of medical intermediate is high. Modified CG can be used as an ideal material for the adsorption treatment of medical intermediate wastewater. Herein, the CG was treated with three activation methods of high-temperature calcination, freezing microwave and acidification treatment to investigate their adsorption behavior to p-hydroxybenzenesulfonic acid. SEM, FTIR, XRD, XPS and BET were used to study the microstructure of raw and modified CG. The relationship between the activation methods and the structure of the CGs was established. The specific surface area of calcined CG increases obviously, which is attributed to the elimination of interlayer water. Acidification treatment can effectively activate the chemical structure of CG surface. By using ultraviolet spectrophotometer, both the kinetics and thermodynamics of the adsorption processes are investigated and fitted with the kinetic equations and adsorption thermodynamic equations. Results indicate that the CG treated with acidification method has the best adsorption effect on p-hydroxybenzenesulfonic acid, and the maximum removal rate reaches 85.34%. The quasi-second-order rate equation and Freundlich model are adopted to analyze the adsorption kinetics and thermodynamics, and results show that the adsorption process includes both physical adsorption and chemisorption. Overall, the relationships of activation method-microstructure-adsorption performance are revealed, which is significant to guide the application of CG in the adsorption field.

Keywords: Coal Gangue, Adsorption, P-hydroxybenzenesulfonic Acid, Modified

INTRODUCTION

CG is the main solid waste resulting from the process of coal mining and washing, which accounts for about 10-25% of total coal production [1]. In the coal industry and enterprises, people have been actively struggling to apply CG in different fields to solve the serious problem of CG accumulation [2]. CG was developed to be used for power regeneration, building materials and land reclamation, leading to a significant increased utilization amount. However, along with the strict environmental regulations, there is an increasing demand for the utilization of CG in a more appropriate and efficient manner. Scientific investigation on the high value-added utilization of CG is of equal importance [3]. For example, the development of CG as an adsorbent has been advocated ascribed to its high porous structure and inter layered clay minerals, which is favorable for absorption properties. Moreover, from the environmental protection and resource conservation points of review, CG is an ideal candidate for common adsorbents, which not only addresses its disposal but also contributes to low material costs and sustainable use of resources. Many scholars have done researches investigating the adsorption properties of CG [4]. However, ascribed to its stable chemical structure, the adsorption capacity of raw CG is limited. Thus the amelioration of adsorption properties of CG is necessary to meet the commercial utilization criterion. Specific treatment processes have adopted CGs to elevate the reactivity for chemical elements, such as mechanical grinding, thermal treatment and chemical activation. The calcination of CG is an effective method for improving the adsorption ability, showing a removal rate of 92.3% for phosphate under the concentration of 10 mg/L. Wang et al. [5] prepared adsorbent from CG by high temperature treatment method, and the final sample presented good adsorption effect on refining wastewater with a best adsorption rate of 49.7%. Guo explored the effect of grinding on the physical properties and chemical structure of gangue. The results showed that with the increase of grinding time, the specific surface area and pore size of gangue were promoted, and ultimately the adsorption performance was elevated. Guo [6] used 1 mol/L HCl solution to activate and modify CG at 100 °C for 150 min, and studied its adsorption performance for Fe^{2+} and Mn^{2+}. While results showed that the acid modification method had poor effect on ameliorating the adsorption performance to metal ions [7]. Tremendous works have been done investigating the effect of modification treatments for gangue on its adsorption properties. However, to the best of our knowledge, little work has been adopted to systematically investigate the effects of different activation methods on the adsorption properties of gangue [8]. Herein, the CG is activated by three modification methods of high temperature calcination, acidification and freezing microwave modification, and their adsorption performances are com-

†To whom correspondence should be addressed.
E-mail: penglonggui@163.com

pared.

Recently, water remediation from pharmaceutical compounds has become now a very actual and demanding task, due to the non predicable threat of the highly hazardous water pollutants to living organism. This paper chose the industrial pharmaceutical waste of benzene derivatives as a medium and investigates the absorption properties for p-hydroxybenzenesulfonic acid by CG. The adsorption performance was quantitatively evaluated from both adsorption kinetics and adsorption thermodynamic mechanism. The influence of activation method on the material structure and adsorption performance was systematically studied.

EXPERIMENT

1. Materials

Raw CG was taken from Binzhou City (Shaanxi Province, China). The CG used in this study was screened by ball milling without any chemical pretreatment, and its particle size was less than 120 mesh (The range of sizes is given in the attachment, Fig. S1). The chemical reagents, such as sulfuric acid (H_2SO_4 98% wt%, Tianjin Fuchen Chemical Reagent Factory), P-hydroxybenzenesulfonate hydrate ($C_6H_6O_4S$, 80% wt%, McLean) and deionized water were used. All chemical agents were analytical grade and the reagents were used as received without further purification.

2. Preparation of CG Modified Materials

The raw CG was treated by high temperature calcination, acidification and freezing microwave modification, respectively. For high temperature calcination, 10 g of CG powder was placed in a crucible, and calcined at 600 °C in box-type resistance furnace for 5 h. Ultimately, the high temperature calcination treated CG was prepared. For acidification treatment; 10 g CG was put into the conical flask, the 98 wt% sulfuric acid solution was diluted to 60%, the water bath temperature was kept at 80 °C under the condition of acid leaching 4 h after taking out, in the blast drying oven 95 °C drying, the second kind of adsorption material; Finally, 10 g CG sample was placed in a low temperature refrigerator and frozen at −20 °C for 10 min. Then the sample was processed by freezing microwave method with a radiation power of 350 W and microwaving for 4 min. The third adsorption material was prepared.

3. Characterization Methods

Through X-ray diffraction (XRD, DX-2700, Japan), in the range of 2θ (5-100°) radiation with Cu Kα, tube voltage 40 kV, tube current 30 mA, scanning range of 5-100°, scanning speed 4°/min, the morphology was characterized by scanning electron microscopy (SEM, SU8020, Hitachi LTD, Japan, operating at 15 KV). The Quadrasorb Station 2 specific surface analyzer was used to measure the specific surface area of the sample. Before the measurement, the sample was degassed at 573 K for 10 hours, and the BET adsorption isotherm was used to measure the specific surface area in the range of relative pressure (P/P_0) 0-1.0. X-ray photoelectron spectroscopy (Shimadzu ULTRA DLD, Al Kα rays, 1,486.6 eV photons) was used to detect the elemental composition of the surface of the sample material. The monochromatic Al Kα rays (1,486.6 eV photons) were used as the X-ray source. The operating voltage was 12 kV and the operating current was 12 mA. The ambient pressure was 2×10^{-7} Pa.

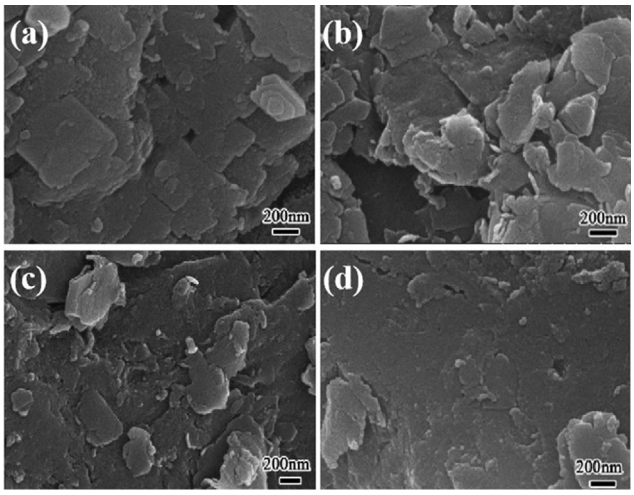

Fig. 1. SEM images of raw CG (a), high-temperature calcined CG (b), acidified CG (c), and frozen microwave treated CG (d).

RESULTS AND DISCUSSION

1. Properties of Modified Coal Gangue

Fig. 1 shows the microstructures of raw and treated CGs which present obvious lamellar structures. According to Fig. 1(a), raw gangue has a relatively compact arranged lamellar structure with small particles irregularly piled together, making it have a certain porosity [12]. After high temperature calcination treatment, the CG becomes more porous and loose, the transformed feature is mainly ascribed to the evaporation of water and the disappearance of carbon in the process of high temperature calcination, thus increasing specific surface area is expected for high-temperature calcined CG [13]. The influence of corrosion in sulfuric acid solution on the microstructure of CG is obvious. Smaller particles can be observed floating on the surface, while the raw multilayer structure is ambiguous. H_2SO_4 would react with the metal elements in the CG materials, such as Al, generating defects and holes within the CG. However, a certain part of the material may continue to overcontact with acid, leading to the collapse of the original multilayer and porous structure [14]. It can be observed in Fig. 1(d) that the morphology of CG treated by freezing microwave method does not change much with relatively flat surface. The possible reason may be that the energy adopted on CG by microwave treatment is not high enough to change the internal structure of CG [15].

Fig. 2(a) presents the XRD diffraction curves of the raw and treated CGs. The raw CG peak at 2θ=10° corresponds to the characteristic diffraction peak of kaolinite, and the peaks at 2θ=12° originate from quartz, which proves that the raw CG mainly contains kaolinite and quartz [16]. By comparing the characteristic spectra of raw and treated CGs, microstructure transition can be expected during the modification processes. It is obvious that the characteristic peak of kaolinite at 2θ=10° in XRD diffraction curve of high-temperature calcined CG disappears, indicating that the kaolinite is totally transformed into metakaolinite with high activity. However, the characteristic diffraction peak of kaolinite in the CGs treated with acidification and frozen microwave method still exists at 2θ=0° [17]. When the CG is treated under 600 °C, kaolinite would

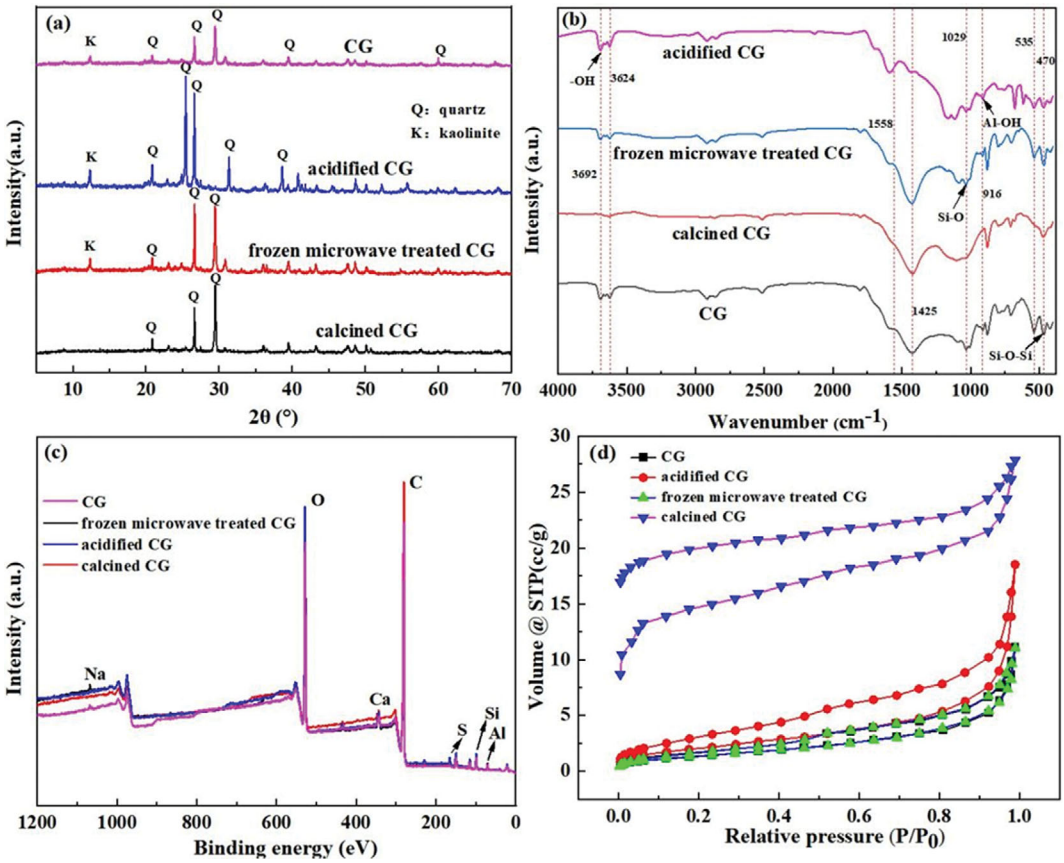

Fig. 2. XRD patterns (a) FTIR spectra (b) XPS spectra (c) and N_2 adsorption-desorption curves (d) of raw and treated CGs.

lose interlayer structural water, resulting in the collapse of interlayer structure. At the same time, the kaolinite is transformed into disordered metakaolinite with the absence of hydroxyl groups, which promoted their reaction activity. When the CG is modified by microwave, the crystalline transformation and phase transformation occur in kaolinite. Microwave is absorbed by the material and converted into heat energy to heat the inside and outside of the object at the same time [18]. By observing the peaks located in the range of 2θ=20°-30°, it can be seen that the characteristic peaks of acidified CG become stronger, which is ascribed to the chemical reaction between CG and H_2SO_4 solution, resulting in the rearrangement of some bond valence structure [19]. This can be further proven by the FT-IR spectrogram in Fig. 2(b).

FT-IR was used to characterize the chemical composition and structure of the raw and treated CGs materials, as shown in Fig. 2(b). In the infrared absorption spectrum of raw CG, the absorption peaks at 3,692 cm^{-1} and 3,624 cm^{-1} correspond to the stretching vibration of hydroxyl groups. The peaks at 1,029 cm^{-1}, 916 cm^{-1}, 535 cm^{-1} and 470 cm^{-1} correspond to the stretching vibration of Si-O, the bending vibration of Al-OH [20], the bending vibration of Si-O-Al and the bending vibration of Si-O-Si, respectively. After high temperature calcination, the stretching vibration absorption peaks of hydroxyl groups at 3,692 cm^{-1} and 3,624 cm^{-1} are significantly weakened, which is mainly ascribed to the absence of interlayer structural water. The Al-OH vibration peak at 916 cm^{-1} disappears, and the vibration peak of Si-O-Al at 535 cm^{-1} weakens significantly. It indicates that the molecular structure of Al-OH and Si-O-Al has been destroyed [21]. In addition, the stretching vibration absorption peak of Si-O disappears at 1,029 cm^{-1}, and the absorption peak of Si-O-Si weakens at 470 cm^{-1}, while a new vibration peak C-O appears at 1,098 cm^{-1}. These results can clearly prove the proposed conclusion that kaolinite is transformed into metakaolinite [22]. After frozen microwave treatment, besides small changes in the strength of some functional groups, few changes can be observed in the FTIR spectrum, indicating that the frozen microwave treatment has no great influence on the chemical structure of CG. The infrared image of acidified CG treatment shows that the bending vibration absorption peak intensity of Si-O-Al at 535 cm^{-1} is weakened, and the Al-O vibration peak disappears at 916 cm^{-1}, which is ascribed to the reduction of the content of Al_2O_3 in CG components after the reaction with acid solution [23]. Therefore, the acidification treatment has a great influence on the chemical structure of CG, while the freezing microwave has the least influence, which is consistent with the XRD analysis results [24].

XPS profiles of raw and treated CGs are shown in Fig. 2(c). As can be seen from the characteristic peaks at 281 eV and 529 eV in the figure, for all CGs, carbon and oxygen are the two main elements. In addition, there is a small amount of sulfur, aluminum, silicon, calcium, and sodium elements, which are mainly reflected in the characteristic peaks of 151 eV and 71 eV. Compared with the spectra curve of raw CG, the peak intensity ratio for carbon to

oxygen element becomes higher for high temperature calcined CG, demonstrating the loss of oxygen. During high temperature sintering process, the elimination of free water on the surface of the material and the interlayer bonding water, as well as oxygen containing functional groups contribute to the decrease of oxygen content. Carbonization occurs in the process of high temperature calcination, leading to the decrease of oxygen element and the increase of carbon-oxygen ratio [25]. Intriguingly, for the CG materials by acidification treatment, the characteristic peak intensities of oxygen and sulfur elements are increased compared with the raw CG, while the characteristic peak intensity of aluminum elements is decreased. This is ascribed that in the process of acidification, sulfate ions react with aluminum and other metal ions contained in CG. Therefore, the intensity of characteristic peaks of oxygen elements and sulfur elements is enhanced [26]. Compared with the original CG, the characteristic peak intensity of oxygen elements decreased after the freezing microwave treatment, because some of the interlayer structured water was volatilized during the microwave treatment after freezing.

The specific surface area of raw and treated CGs was tested by N_2 physical adsorption instrument, and the results are shown in Fig. 2(d). According to the six adsorption isotherms classified by the International Union of Pure and Applied Chemistry (IUPAC), all the four kinds of CGs in Fig. 2(d) yield atype IV adsorption isotherm model, indicating the existence of mesoporous structure in the material [27]. BET method was used to test the specific surface area data of raw CG, CG calcined at high temperature, CG treated by acidification and CG treated by cryomicrowave. The specific surface areas for raw CG, high-temperature calcined CG, acidified CG and frozen microwave treated CG are 5.119, 55.361, 7.703 and 5.141 m^2/g, respectively. It is notable that after the thermal modification of CG, the specific surface area for CG was significantly enhanced, which is favorable for absorption properties. The elements of Al, Fe, Ca and other substances existing in raw CG would react with acid solution, resulting to micro-voids [28]. However, attributed to the collapse of the original multilayer and porous structure observed in the SEM image, the final specific surface area for acidified CG is only slightly increased. Mesoporous of different shapes and sizes are represented as hysteresis rings of different shapes and sizes on the isotherm [29].

2. Adsorption Kinetics of Activated Coal Gangues

The adsorption kinetics curves of the activated CG on p-hydroxybenzenesulfonic acid are shown in Fig. 3(a). It is demonstrated that the removal rate increases with the continuous growth of adsorption time for all the CG. When reaching a certain point, the growth rate starts to slow and the trend becomes gentle. Impressively, the CG modified by acidification presented the best adsorption performance with the highest adsorption rate of 85.34%. It is at a high level compared with other materials (Table S1, see the attachment). Despite the fact that high temperature calcined CG endows the highest specific area, it only presents a medium adsorption performance, with the highest adsorption rate of 78.70%. While the CG modified by freezing microwave has only 75.94% removal rate of the organic matter. Therefore, the CG modified by sulfuric acid shows the best adsorption performance. The possible reason may be that the interlayer charge density increases for acidified CG as a result

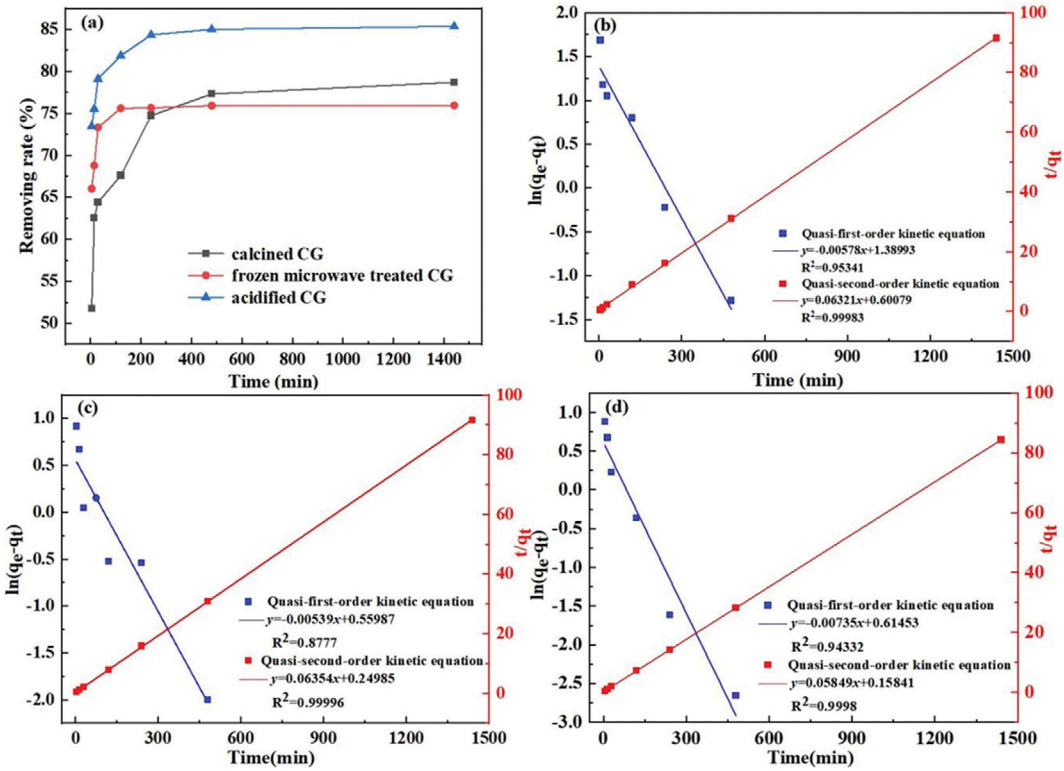

Fig. 3. Adsorption kinetic curves of activated CGs for p-hydroxybenzenesulfonic acid (a) and kinetic fitting results of high-temperature calcined CG (b), frozen microwave treated CG (c) and acidified CG (d).

Table 1. The Parameters for p-hydroxybenzoesulfonic acid on the basis of pseudo-1st-order and pseudo-2nd-order kinetic models

Samples	Pseudo-1st-order kinetic model		Pseudo-2nd-order kinetic model	
	K_1 (min^{-1})	R^2	K_2 (g/mg/min)	R^2
Calcined CG	5.78×10^{-3}	0.95341	6.321×10^{-2}	0.99983
Frozen microwave treated CG	5.39×10^{-3}	0.8777	6.354×10^{-2}	0.99996
Acidified CG	7.35×10^{-3}	0.94332	5.849×10^{-2}	0.9998

of protonating, which can enhance the interaction between CG and p-hydroxybenzenesulfonic acid since it is an ionic compound [30]. Therefore, the elevated adsorption process of p-hydroxybenzenesulfonic acid by acidified CG mainly comes from the electrostatic interaction between CG and p-hydroxybenzenesulfonic acid [31]. The adsorption behavior of high-temperature calcined CG is slightly better than that of freezing-microwave treated CG, which is to the fact that the increase of specific surface area is conducive to providing more adsorption sites. However, it is that in the process of calcination [32]. It is intriguing to find that in the initial stage of the adsorption process, the adsorption rate of CG samples treated by freezing microwave is greater than that of high-temperature calcined CG. As time goes on, the adsorption efficiency is gradually surpassed by calcined CG [33]. The possible reason may be that during the high temperature calcination process, some oxygen-containing functional groups are removed from the surface of CG, which is negative to the interaction between high temperature calcined CG and p-hydroxybenzenesulfonic acid. However, after a period of adsorption, most of the adsorption sites in the frozen microwave treated CG were occupied and the adsorption rate began to decrease, while for high temperature calcined CG more adsorption sites were generated as a result of the increased specific surface area [34]. Therefore, in the adsorption process, both the interaction between the adsorbent and the adsorbed and adsorption sites play very important roles in the adsorption behavior [35].

To explore the influence of activation methods on the adsorption rate during the whole adsorption process, the quasi-first-order kinetic equation (Eq. (4), see the attachment) and quasi-second-order rate equation (Eq. (5)) are used to analyze the adsorption process [36]. Results are shown in Fig. 4. The fitting results show that the adsorption processes of all the activated CGs are in good line with the quasi-second-order rate equation according to the correlation coefficient R^2 value (according to Table 1), indicating that the adsorption processes include the external liquid film diffusion process, the surface adsorption process and the internal particle diffusion process [37]. When the modified CG enters the p-hydroxybenzoesulfonic acid solution, the p-hydroxybenzoesulfonic acid molecules can quickly reach the surface of the CG adsorption material, so the adsorption rate is fast. When the adsorption sites on the CG surface are gradually occupied, the p-hydroxybenzoesulfonic acid molecules in the solution slowly diffuse in the surface of modified CG, the adsorption rate starts to decline [38]. The whole adsorption process can be divided into three stages: rapid adsorption, medium adsorption and equilibrium adsorption. The first stage is the membrane diffusion of p-hydroxybenzoesulfonic acid on the surface of the modified CG. The second stage is the particle diffusion of p-hydroxybenzoesulfonic acid on the modified CG, and the third stage is internal diffusion. It can be found that in the first 100 min, the adsorption performance of frozen microwave treated CG is faster than that of high temperature calcined CG. In the initial adsorption process, the adsorption process is mainly controlled by the first and second stages, which is closely related to the static interaction between CG and p-hydroxybenzoesulfonic acid [39]. Ascribed to the loss of oxygen-containing functional groups during high temperature calcination treatment process, a weaker molecular interaction between calcined CG and p-hydroxybenzoesulfonic acid is formed, leading to a slower adsorption process. However, the removal rate of calcined CG gradually surpasses frozen microwave treated CG after 345 min, because the maximum removing rate of p-hydroxybenzoesulfonic acid mainly depends on the total amount of adsorption sites. Since the calcined CG endows a higher specific aera, a larger removing rate can be reached.

3. Adsorption Thermodynamics of Activated Coal Gangues

Fig. 4 shows the adsorption isotherm of activated CGs to p-hydroxybenzenesulfonic acid. When different CGs are used to adsorb p-hydroxybenzenesulfonic acid solution, the same trend is observed, that is, at the stage of low solution concentration, the adsorption capacity increases proportionally with increasing p-hydroxybenzenesulfonic acid concentration, while with continuously increasing, the adsorption capacity is enhanced with a slow trend [40]. It is worth noting that it is until 40 mg/L for the acidified CG, that the increment of adsorption capacity slows, while for the frozen microwave treated CG, it starts at the concentration of 30 mg/L, which can also reflect the excellent adsorption performance of acidi-

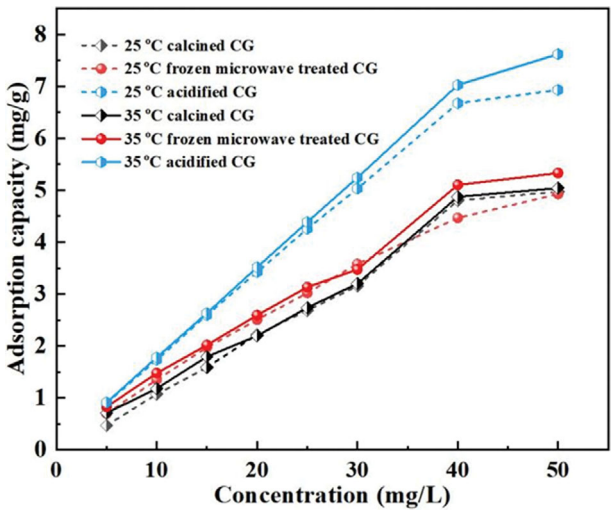

Fig. 4. Adsorption isotherm of p-hydroxybenzenesulfonic acid at 25 °C and 35 °C.

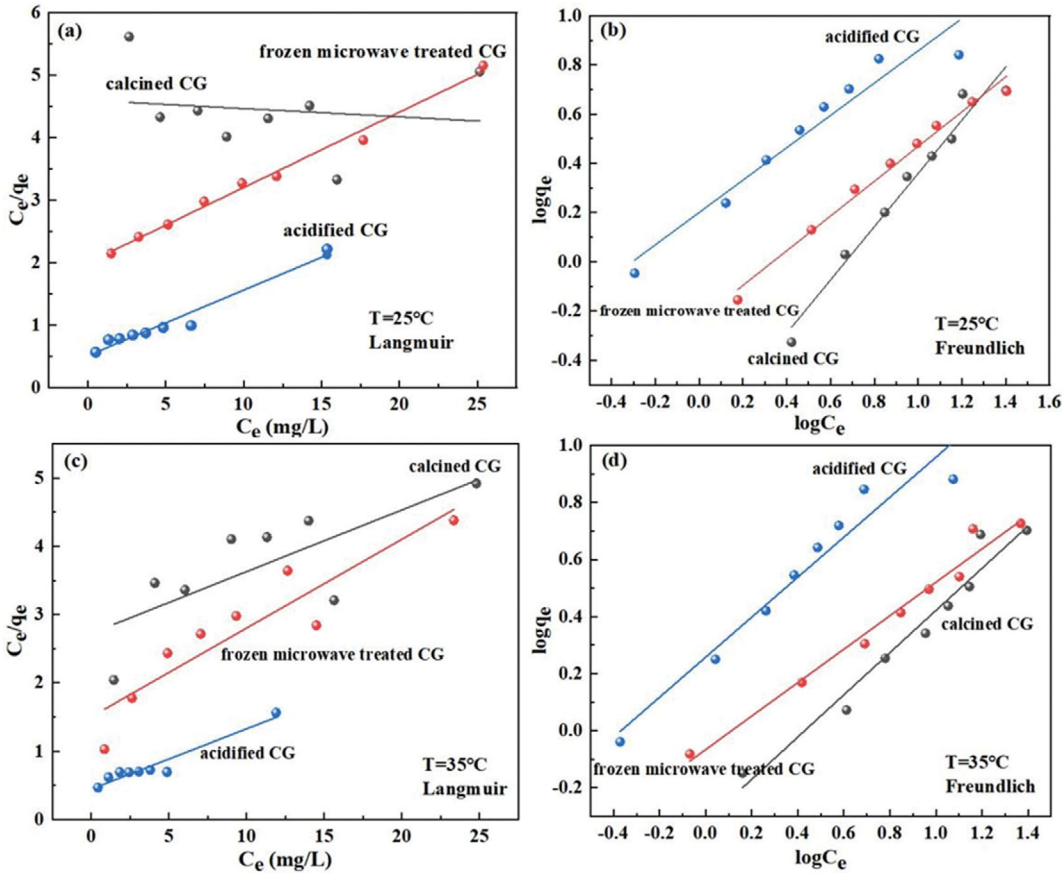

Fig. 5. Isothermal simulation in activated CGs for the adsorption of p-hydroxybenzenesulfonic acid at 25 °C by Langmuir model (a) and Freundlich model (b) and at 35 °C Langmuir model (c) and Freundlich model (d).

Table 2. Related parameters of Langmuir and Freundlich adsorption isotherm models

Samples	T (K)	Langmuir				Freundlich			
		Fitted equation	q_{max}	K_L (L/mg)	R^2	Fitted equation	K_F (L/mg)	n	R^2
Calcined CG	298	y=0.03429x+4.14244	29.16	0.008	0.906	y=1.082x−0.72262	0.18	0.92	0.963
	308	y=0.06221x+3.36124	7.15	0.094	0.922	y=0.73928x−0.31765	0.48	1.35	0.952
Microwave frozen treated CG	298	y=0.12046x+1.99775	7.56	0.074	0.990	y=0.7522x−0.2655	0.55	1.33	0.995
	308	y=0.11966x+1.79293	8.37	0.067	0.917	y=0.58622x−0.06581	0.65	1.70	0.972
Acidulated CG	298	y=0.04691x+0.70137	21.32	0.067	0.950	y=0.7873x+0.17069	1.48	1.27	0.994
	308	y=0.09246x+0.44278	10.82	0.209	0.980	y=0.83039x+0.23836	1.72	1.20	0.991

fied CG. In the low concentration range, the temperature has no great influence on the adsorption capacity of p-hydroxybenzenesulfonic acid, and in the high concentration range, the adsorption capacities are influenced by the temperature more obviously [41,42].

Both Langmuir (Eq. (6), see the attachment) and Freundlich isothermal model (Eq. (7), see the attachment) are used to analyze the thermodynamic of adsorption processes. The fitting results are shown in Fig. 5 and Table 2.

According to Fig. 5 and Table 2, for the three modified CGs, the Freundlich model is more suitable to describe the adsorption process of the three modified CG on p-hydroxybenzoesulfonic acid, judging from the linear fitting correlation coefficient R^2 of the Langmuir model and Freundlich model [43]. The whole adsorption process is neither a single molecule layer adsorption nor a simple chemisorption process, but the results of physical adsorption and chemisorption [44]. For the Langmuir simulation result, the K values for high temperature calcined CG and acidification treated CG are 0.094 and 0.209 for 35 °C, which are both larger than those of 25 °C, indicating that the adsorption system is more stable at 35 °C. Thus, it can be concluded that the increase of temperature is conducive to the adsorption performance of calcined CG and acidized CG, which may be because heating can increase the diffusion rate of p-hydroxybenzoesulfonic acid in the solution, so that it can move faster to the surface of the adsorbent [45]. While for the adsorption process of frozen microwave treated CG, an opposite trend is observed, that is, the adsorption process is more stable at

25 °C, which may because low temperature is favorable for the static interaction between CG and p-hydroxybenzoesulfonic acid. In Freundlich, the adsorption characteristic coefficient n of high-temperature calcined samples at 25 °C is 0.92 (<1), indicating that the adsorption process for temperature calcined CG is more likely to occur at 35 °C [46]. The adsorption characteristic coefficient n values of freezing microwave and acidified samples at 25 °C and 35 °C are both greater than 1 (1≤n≤10), which can prove the strong interaction between these two CG with p-hydroxybenzoesulfonic acid. Generally, chemical adsorption happens in the high-temperature calcined samples at higher temperature, while for freezing microwave and acidified samples, the chemical adsorption process is not influenced by temperature.

CONCLUSIONS

Overall, CG was modified by three methods of high temperature calcination, acidification and frozen microwave treatment. The specific surface area increased under high temperature calcination, while oxygen-containing functional groups on the surface were lost. The acidification treatment leads to the activation of the chemical structure in the CG surface. However, the specific surface area and chemical structure of frozen microwave treated CG have little change. The acidified CG shows the best adsorption performance because of the strong electrostatic attraction to p-hydroxybenzenesulfonic acid. Although the high temperature calcined CG has large specific surface area, the loss of surface oxygen-containing functional groups during calcination is not conducive to strong electrostatic attraction, leading to poor adsorption performance in the initial stage of the adsorption process. However, its larger specific surface area can contribute more adsorption sites, which is favorable for the continuous adsorption process and achieving a higher maximum adsorption rate. Therefore, during the treatment of CG, the increase of surface charge density and specific surface area have a strong effect on the whole adsorption process. It can be conjectured that with proper modification treatment, the adsorption performance of CG can be elevated effectively, which is promising for the application of CG in the treatment of medical wastewater.

SUPPORTING INFORMATION

Additional information as noted in the text. This information is available via the Internet at http://www.springer.com/chemistry/journal/11814.

REFERENCES

1. Q. Lu, X. F. Dong, Z. W. Zhu and Y. C. Dong, *J. Hazard. Mater.*, **273**, 136 (2014).
2. Y. L. Huang, J. M. Li, D. Ma, H. D. Gao, Y. C. Guo and S. Y. Ouyang, *Total Environ.*, **693**, 133607 (2019).
3. B. Jablonska, A. V. Kityk, M. Busch and P. Huber, *J. Environ. Manage.*, **190**, 80 (2017).
4. M. Zhou, Y. W. Dou, Y. Z. Zhang, Y. Q. Zhang and B. Q. Zhang, *Constr. Build Mater.*, **220**, 386 (2019).
5. L. P. Zhang, A. L. Chen, H. B. Qu, S. Q. Xu, X. Zhang and X. W. He, *Water Sci. Technol.*, **72**, 1940 (2015).
6. Y. X. Guo, K. Z. Yan, L. Cui and F. Q. Cheng, *Powder Technol.*, **302**, 33 (2016).
7. J. Geng, M. Zhou, T. Zhang, W. Wang, T. Wang, X. Zhou, X.Wang and H. Hou, *Mater. Struct.*, **50**, 1 (2017).
8. Y. C. Hu, W. Q. Liu, Y. D. Yang, M. Y. Qua and H. L. Li, *Chem. Eng. J.*, **359**, 604 (2019).
9. Z. Zhang, V. V. Pendin, W. J. Feng and Z. Q. Zhang, *Sci. Cold Arid. Reg.*, **7**, 199 (2015).
10. F. Q. Gan, J. M. Zhou, H. Y. Wang, C. W. Du and X. Q. Chen, *Water Res.*, **43**, 2907 (2009).
11. F. Haghseresht, S. B. Wang and D. D. Do, *Appl. Clay Sci.*, **46**, 369 (2009).
12. S. L. Tian, P. X. Jiang, P. Ning and Y. H. Su, *Chem. Eng. J.*, **151**, 141 (2009).
13. B. B. Qiu and F. Duan, *Colloid Surf. A*, **571**, 86 (2019).
14. L. Zhou, H. J. Zhou, Y. X. Hu, S. Yan and J. L. Yang, *J. Environ. Manage.*, **234**, 245 (2019).
15. X. L. Sun, L. Zhang, Z. X. Xie, B. Li and S. Y. Liu, *J. Surfactants Deterg.*, **24**, 269 (2021).
16. U. T. Gonzenbach, A. R. Studart, E. Tervoort and L. J. Gauckler, *J. Am. Ceram. Soc.*, **90**, 16 (2007).
17. H. B. Zhao, T. Wang, H. Zhang, Y. Li and Z. Q. Wei, *J. Pet. Sci. Eng.*, **174**, 553 (2019).
18. F. X. Song, N. Wang, Z. Z. Hu, Z. Zhang, X. X. Mai, W. B. Jie and L. Bin, *Appl. Water Sci.*, **11**, 1 (2021).
19. B. K. Aziz, Dler M. Salh SHwan and S. Kaufhold, *Silicon*, **14**, 893 (2022).
20. T. Xiong, X. Z. Yuan, H. Wang, Z. B. Wu and L. B. Jiang, *Chem. Eng. J.*, **366**, 83 (2019).
21. W. X. Zhu, H. Song, C. M. Jia and S. Yao, *J. Cent. South Univ.*, **21**, 2832 (2014).
22. S. Yan, P. G. He, D. C. Jia, Q. G. Wang, J. J. Liu, J. L. Yang and Y. Huang, *Int. J. Appl. Ceram. Technol.*, **15**, 1602 (2018).
23. H. Zhou, M. S. Zhang and S. F. Sun, *Sci. Adv. Mater.*, **13**, 2157 (2021).
24. R. Mohammadi, A. Azadmehr and A. Maghsoudi, *Sep. Sci. Technol.*, **55**, 3343 (2020).
25. S. Yan, F. Y. Zhang, L. Wang, Y. D. Rong, P. G. He and D. C. Jia, *J. Environ. Manage.*, **246**, 174 (2019).
26. Y. B. Zhang, Y. T. Zhang, X. Q. Shi, Y. Q. Li and X. D. Zhang, *Fuel*, **315**, 123275 (2022).
27. X. L. Wang and Y. Zhang, *Sci. Adv. Mater.*, **11**, 277 (2019).
28. J. M. Li, Y. L. Huang, W. Li and Y. C. Guo, *J. Clean Prod.*, **329**, 129756 (2021).
29. O. S. Nuri, M. Irannajad and A. Mehdilo, *J. Mol. Liq.*, **291**, 111311 (2019).
30. M. Manono, K. Corin and J. Wiese, *Minerals*, **9**, 231 (2019).
31. S. Ahmadzadeh, A. Asadipour and M. Yoosefian, *Desalin. Water Treat.*, **92**, 160 (2017).
32. D. M. Salh, B. K. Aziz and S. Kaufhold, *Silicon*, **12**, 87 (2020).
33. G. Z. Nie, S. J. Qiu, X. Wang, Y. Du and Q. R. Zhang, *Chinese Chem. Lett.*, **32**, 2342 (2021).
34. H. K. Zhang, X. R. Zhang, J. F. Liu and L. M. Zhang, *J. Environ. Manage.*, **314**, 115044 (2022).
35. M. M. Fawzy, H. M. Salem and A. H. Orabi, *Hydrometallurgy*, **213**,

105940 (2022).
36. B. Jabłońska, A. V. Kityk, M. Busch and P. Huber, *J. Environ. Manage.*, **190**, 80 (2017).
37. R. Mohammadi, A. Azadmehr and A. Maghsoudi, *J. Environ. Chem. Eng.*, **9**, 105003 (2021).
38. Y. Wu, Z. J. Wu, K. Liu, F. Li, Y. J. Pang and J. B. Zhang, *Korean J. Chem. Eng.*, **37**, 1786 (2020).
39. R. Mohammadi, A. Azadmehr and A. Maghsoudi, *J. Environ. Chem. Eng.*, **7**, 103494 (2019).
40. G. T. H. Ooi, K. Tang, R. K. Chhetri, K. M. S. Kaarsholm and K. Sundmark, *Bioresour. Technol.*, **267**, 677 (2018).
41. N. J. Bu, X. M. Liu, S. L. Song, J. H. Liu and Q. Zhen, *Adv. Powder Technol.*, **31**, 2699 (2020).
42. Z. M. Puyen, E. Villagrasa, J. Maldonado, E. Diestra and I. Esteve, *Bioresour. Technol.*, **126**, 233 (2012).
43. J. M. Zhu, S. H. Guo and X. H. Li, *RSC Adv.*, **5**, 103656 (2015).
44. H. D. Qin, R. Xiao, R. H. Zhang and J. Chen, *Water Sci. Technol.*, **2017**, 686 (2018).
45. J. M. Zhou, Y. S. Fu, M. Y. Zhang, Y. Q. Liu, S. H. Ding and L. Zhao, *Desalin. Water Treat.*, **211**, 229 (2021).
46. M. Han, Z. W. Zhao, W. Gao and F. Y. Cui, *Bioresour. Technol.*, **145**, 17 (2013).

Supporting Information

Investigation on the adsorption performance of modified coal gangues to p-hydroxybenzenesulfonic acid

Longgui Peng†, Rong Wang, Huanquan Cheng, Liangqing Zhang, Yugang He, Chenghui Yin, and Xin Zhang

College of Materials Science & Engineering, Xi'an University of Science and Technology, Xi'an, 710054, China
(*Received 1 December 2022 • Revised 3 February 2023 • Accepted 5 February 2023*)

S1. Materials

The particle size of CG was less than 120 mesh; the exact size or range of sizes was given as follows.

S2. Adsorption Experiment

S2-1. p-Hydroxybenzenesulfonic Acid Adsorption Experiment

The prepared CG samples were used as adsorbent, and 0.5 g of

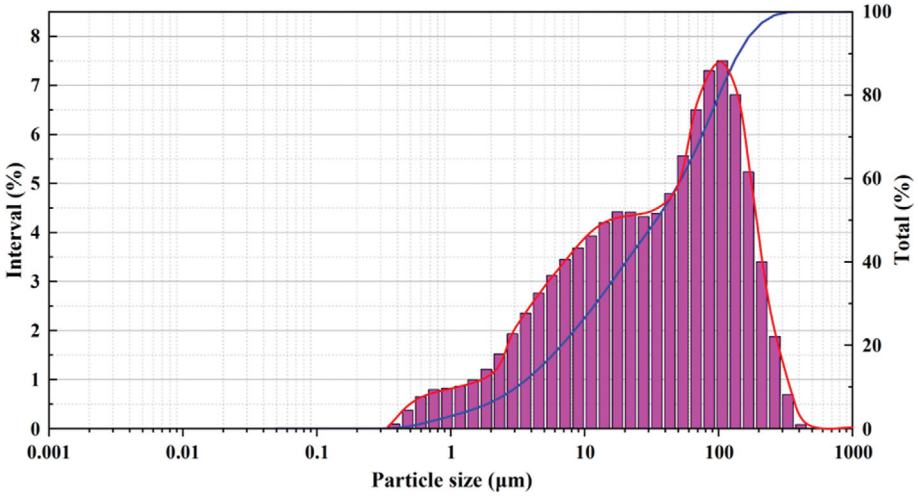

Fig. S1. Grain size distribution of coal gangue in materials.

Table S1. Size distribution table of coal gangue in materials

Particle size (μm)	Interval (%)	Total (%)	Particle size (μm)	Interval (%)	Total (%)	Particle size (μm)	Interval (%)	Total (%)
0.05	0	0	1.85	1.21	5.78	68.01	6.5	67.11
0.06	0	0	2.31	1.52	7.3	85.21	7.3	74.41
0.08	0	0	2.90	1.93	9.23	106.70	7.5	81.91
0.10	0	0	3.63	2.35	11.58	133.70	6.81	88.72
0.12	0	0	4.55	2.76	14.34	167.50	5.23	93.95
0.15	0	0	5.70	3.12	17.46	209.90	3.4	97.35
0.19	0	0	7.14	3.45	20.91	263.00	1.88	99.23
0.24	0	0	8.94	3.68	24.59	329.50	0.69	99.92
0.30	0	0	11.20	3.93	28.52	412.80	0.08	100
0.38	0.09	0.09	14.03	4.2	32.72	517.20	0	100
0.48	0.37	0.46	17.58	4.42	37.14	647.90	0	100
0.60	0.65	1.11	22.03	4.41	41.55	811.80	0	100
0.75	0.79	1.9	27.60	4.32	45.87	1,017.00	0	100
0.94	0.82	2.72	34.58	4.39	50.26	1,274.00	0	100
1.18	0.86	3.58	43.33	4.79	55.05	1,596.00	0	100
1.47	0.99	4.57	54.28	5.56	60.61	2,000.00	0	100

the above three kinds of CG modified adsorption materials were respectively taken into 100 ml, 100 ppm p-hydroxybenesulfonic acid solution, and oscillated at 25 °C for 5 min, 15 min, 30 min, 2 h, 4 h, 8 h, 24 h, respectively. The removal rate was calculated by the formula. Under the conditions of 25 °C and 35 °C, 5 ppm, 10 ppm, 15 ppm, 20 ppm, 25 ppm, 30 ppm, 40 ppm and 50 ppm p-hydroxybenzenesulfonic acid were adsorbed for 24 h, and the adsorption capacity was calculated by formula (1). The initial concentration of the solution was used as the independent variable and the equilibrium adsorption (q_e) was used as the dependent variable.

S2-2. Adsorption Kinetics Fitting

0.5 g of activated CG material was put into the test bottle, and a certain amount of adsorption solution was removed in the test bottle of 100 mL. The supernatant was separated in the centrifuge after shaking at 25 °C for different times, and the absorbance was measured by UV spectrophotometer, and the concentration of p-hydroxybenzenesulfonic acid in the solution was calculated. Eqs. (1) and (2) were used to calculate the adsorption capacity and removal rate.

S2-3. Adsorption Thermodynamic Fitting

Respectively according to three kinds of activated CG materials 0.5 g in a 100 mL bottle test, respectively by pipetting guns take a certain amount of different concentration of solution in the test in the bottle, at 25 °C and 35 °C under the condition of oscillation periods of time, in the centrifuge separation after supernatant fluid, absorbance is measured with ultraviolet spectrophotometer, calculation of hydroxy benzene sulfonic acid concentration in the solution, Eqs. (1) and (2) were used to calculate the adsorption capacity and removal rate [9].

The adsorption capacity formula and removal rate formula are as follows:

$$q=(c_0-c_e)v/1{,}000\ m \quad (1)$$

Where "c_0" is the adsorption capacity of adsorbent, mg/g, "c_e" is Mass concentration of organic matter in solution before adsorption, mg/L, "v" is the volume of the adsorbed solution, mL,"m" is the amount of adsorbent [10].

The calculation formula of removal rate is as follows,

$$Q=(c_0-c_e)/c_0 \quad (2)$$

Where "c_0" is the removal rate of adsorbent, "c_0" is the mass concentration of organic matter in solution before adsorption, "c_e" is the mass concentration of organic matter in the adsorbed solution.

S2-4. Fitting of Standard Curve of p-Hydroxybenzenesulfonic Acid Solution

Absorb a certain amount of 100 ppm concentration of p-hydroxybenzenesulfonic acid solution in the cuvette, to deionized water scanning map reference sample, in the ultraviolet spectrophotometer using the wavelength range of 190-1,100 nm wavelength scanning, the best absorption wavelength of p-hydroxybenzenesulfonic acid is 271 nm.

Different concentrations (5 ppm, 10 ppm, 15 ppm, 20 ppm, 25 pm, 30 ppm, 40 ppm, 50 ppm) of p-hydroxybenzenesulfonic acid solution 5 mL, placed in the ultraviolet spectrophotometer for absorbance scanning measurement [11]. With absorbance as abscissa and each concentration of solution as ordinate, the standard curve of p-hydroxybenzenesulfonic acid was drawn and fitted to obtain R^2, as shown in Fig. 2.

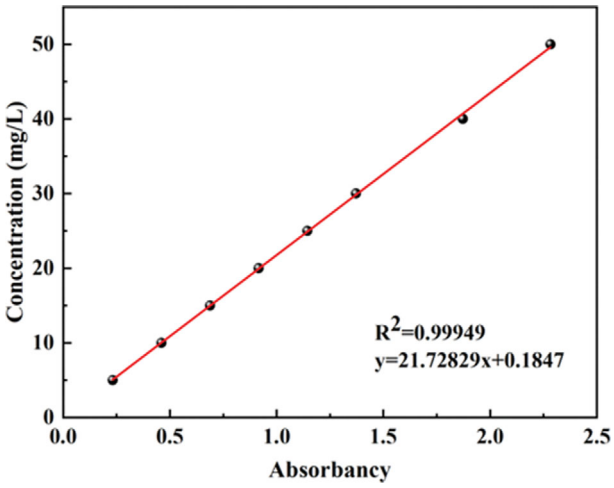

Fig. S2. Standard curve of p-hydroxybenzenesulfonic acid solution.

As shown in Fig. 1, the correlation coefficient R^2 of the standard curve of p-hydroxybenzenesulfonic acid is 0.99949, and the equation of the standard curve is y=21.72829 x+0.1847 (3).

Where "x" is absorbance of p-hydroxybenzenesulfonic acid solution, "y" is the concentration of p-hydroxybenzenesulfonic acid solution in the solution. Therefore, in the subsequent analysis of adsorption kinetics and adsorption thermodynamics, the concentration of residual P-hydroxybenzenesulfonic acid can be calculated from Eq. (3), and then the removal rate can be calculated.

S2-5. Dynamic Adsorption Model

There are three commonly used kinetic models: quasi-first-order kinetic model, quasi-second-order kinetic model and particle diffusion kinetic model. In the study of adsorption behavior, we use adsorption kinetics to explore the adsorption mechanism and control the adsorption rate. The quasi-first-order dynamic equation is as follows:

(1) Quasi-first-order dynamic equation:

$$\ln(q_e-q_t)=\ln q_e-k_1t \quad (4)$$

Where "q_e" is adsorption capacity at equilibrium; "t" is adsorption time; "q_t" represents adsorption capacity at the time of t, mg/g; "k_1" is the first-order adsorption rate constant.

(2) Quasi-second-order dynamic equation:

$$t/q_t=1/(k_2*q_e^2)+(1/q_e)*t \quad (5)$$

Where "q_e" is adsorption capacity at equilibrium, "t" is adsorption time, "q_t" is adsorption capacity at the time of t, "k_2" is the second-order adsorption rate constant. Among them, the kinetic constant k_2 is an important parameter to judge the adsorption rate.

S2-6. Thermodynamic Model of Adsorption

(1) Langmuir isotherm

$$c_e/q_e=(1/kq_{max})+(c_e/q_{max}) \quad (6)$$

The equilibrium concentration of c_e adsorbent, Adsorption capacity at q_e equilibrium, q_{max} saturated adsorption capacity, adsorption equilibrium constant.

Table S2. Adsorption ability of benzene organics by adsorbent materials

Adsorbents	Adsorbates	Capacity	Ref.
MPHAC (activated carbon produced from pomegranate husk)	4CP (4-chlorophenol)	183.64±17.85 mg/g	[1]
MOF-177	Ethylbenzene and Xylenes	250 mg/g	[2]
R001	BSA (Benzenesulfonic acid)	4.35 mmol/g	
R005	BA (Benzoic acid)	4.44 mmol/g	[3]
R003	PH (Phenol)	1.98 mmol/g	
Polyaniline	Trimellitic (Tri)	209.64 mg/g	
	Hemimellitic (Hemi)	143.68 mg/g	[4]
	Pyromellitic (Pyro) acids	267.38 mg/g	
Nitrogen-containing activated carbon	Benzoic acid	340 mg/g	[5]
Molecular imprinted polymers	Benzoic acid	41 mg/g	[6]
MOF-Cu adsorbent	Benzoic Acid (BA)	636.73 mg/g	[7]
	Phenol contaminants	524.42 mg/g	
Hydroxyapatite (HAp) nanopowders	Phenol	10.33 mg/g	[8]
Sodium lignosulfonate modified polystyrene (SLPS)	Phenol	31.08 mg/g	[9]
The CG treated with acidification	p-Hydroxybenzenesulfonic acid	85.34 mg/g	This work

The Langmuir isothermal model is a monolayer adsorption model, and the larger the value of k, the stronger the adsorption performance of the adsorbent. In addition, if the size of k increases with the increase of temperature in the adsorption process, the preliminary conclusion is that the surface adsorption process is endothermic reaction, which belongs to chemisorption. Otherwise, it is an exothermic process, which belongs to physical adsorption.

(2) Freundlich adsorption isotherm

$$\lg q_e = \lg K_F + (1/n) \lg C_e \quad (7)$$

Where "C_e" is the equilibrium concentration, "q_e" is adsorption capacity at equilibrium, "K_F" is Freundlich constant, "n" is adsorption characteristic coefficient.

The characteristic coefficient of adsorption is often used as the judgment basis to judge the degree of difficulty of adsorption: when $n<0.5$, the adsorption process is difficult to carry out, difficult to adsorb; When $1\leq n\leq 10$, it indicates that the adsorption process is easy to proceed, and the larger n is, the stronger the interaction between adsorbent and adsorbent is.

S2-7. The Adsorption Ability of Several Materials to Benzene Organics

REFERENCES

1. S. Hadi, E. Taheri and M. M. Amin, *Chemosphere*, **270**, 128623 (2021).
2. K. Yang, F. Xue and Q. Sun, *J. Environ. Chem. Eng.*, **1**(4), 713 (2013).
3. Y. Sun, Y. Gu and H. Zhang, *J. Environ. Chem. Eng.*, **9**(5), 106026 (2021).
4. M. Laabd, H. Chafai and A. Essekri, *Sustain. Mater. Technol.*, **12**, 35 (2017).
5. H. Qin, R. Xiao and R. Zhang, *Water Sci. Technol.*, **2017**(3), 686 (2018).
6. Z. Yang, H. Wang and H. Sun, *Water Sci. Technol.*, **81**(10), 2176 (2020).
7. V. Pirouzfar, S. N. Moghaddam and S. A. H. S. Mousavi, *J. Contaminant Hydrol.*, **249**, 104048 (2022).
8. K. Lin, J. Pan and Y. Chen, *J. Hazard. Mater.*, **161**(1), 231 (2009).
9. K. Yang, J. Xing and J. Chang, *Polymers*, **12**(11), 2496 (2020).